The 5th European sCO2 Conference for Energy Systems
March 14-16, 2023, Prague, Czech Republic

2023-sCO2.eu-120

PARAMETRIC ANALYSIS OF HEAT EXCHANGER DESIGN IN A TECHNO-ECONOMIC OPTIMIZATION OF A SCO2 SYSTEM.

Thiago Gotelip*
Technische Universität Dresden
Dresden, Germany
Email: Thiago.Gotelip_Correa_Veloso@tu-dresden.de

Uwe Gampe
Technische Universität Dresden
Dresden, Germany

Sebastian Rath
Technische Universität Dresden
Dresden, Germany

Andreas Jäger
Technische Universität Dresden
Dresden, Germany

Stefan Glos
Siemens Energy AG
Mülheim, Germany

ABSTRACT

The investigation of favorable operating conditions for sCO_2 cycles for waste heat recovery is a process that requires a proper analysis of operating parameters, component design, and economic performance. In this aspect, examining the heat exchanger has preponderant significance. In this study, as part of the Carbosola project, a thermoeconomic multiobjective optimization of the sCO_2 cycle is analyzed based on a one-dimensional design of the heat exchangers, focusing on the recuperator. The main objective is to investigate the effect of the non-linearity of the CO_2 properties in the heat exchanger geometry and on the cycle performance. The results highlight the significance of the one-dimensional investigations in the optimization process, while sensitivity analyses indicate the recuperator as key equipment for the optimal cycle operation. Furthermore, the examination reveals the influence of the CO_2 properties characteristics at different operating ranges and its effects on the system's equipment design and thermo-economic performance. Finally, the results indicate a prominent potential of the sCO_2 Preheating architecture for heat recovery from gas turbines.

INTRODUCTION

The more recent development of the supercritical carbon dioxide (sCO_2) power cycle has enhanced its potential for efficient power generation. Especially for waste heat recovery applications, sCO_2 systems stand out as a technically and economically competitive alternative for gas turbine bottoming cycles.

According to Huck *et al.*[1] sCO2 can outperform the steam bottoming cycle at more feasible pressure levels (250) bar for operation temperatures of 500 °C. The sCO_2 power cycle for waste heat recovery (WHR) from a gas turbine can achieve higher efficiency than a steam/water cycle, despite its simplicity and compactness [2].

Li *et al* [3] propose a comparative investigation on the supercritical carbon dioxide power cycle for waste heat recovery of gas turbine is carried out. The results indicate that turbine dominates the investment cost of power cycle. The partial heating cycle is recommended due to its balanced overall performance. Ancona *et al* [4] investigated sCO_2 potential as bottoming recovery cycles in combined heat and power plant configuration comparing several gas turbines models at part-load operation.

Heat exchangers are an enabling technology for efficient power generation with a closed, recuperated Brayton cycle using supercritical carbon dioxide (sCO_2) as the working fluid. Heat exchangers influence the overall system efficiency and system size. The heat exchanger designs must balance between heat exchanger effectiveness and pressure drop to achieve the desired tradeoff between system efficiency and system size. This tradeoff between system efficiency and system size will vary with each energy conversion system application.[5]

Guo [6] employed a segmental design method to accurately capture the drastic variations of properties in the supercritical carbon dioxide (sCO_2) recuperator. According to the authors, both fluids' local heat capacity flow rates have drastic changes in sub-heat exchangers, even though the mass flow rates of both fluids remain unchanged. The segmented method for heat exchangers is largely applied to investigate sCO_2 applications. [7–9]

The thermodynamic properties suffer significant variations near the critical point, and the determination of these characteristics in this region as transfer and pressure drop of carbon dioxide (CO_2) are difficult to predict. These are crucial issues for the design of the cycle. The investigations in [10–12] also present the characteristics of the sCO_2 cycle near the pseudo-critical point.

* corresponding author(s)

DOI: 10.17185/duepublico/77280

Kwon [7] developed a model for PCHE off-design quasi-steady state performance for the recuperator and pre-cooler in a supercritical CO_2 (sCO_2) Brayton cycle, respectively, to optimize power system operation strategies under off-design conditions. The developed model evaluates the performance of the sCO_2 system to establish operation strategies such as inventory control and heater bypass control under off-design conditions.

The present investigation is part of the CARBOSOLA project. The project aims to design the components and system of a technology demonstrator for waste heat recovery applications, besides investigating the methods required for further technology development up to commercial maturity.

METHODOLOGY

The thermal source investigated in this study is the waste exhaust gas from two SGT-A65 gas turbines. Heat recovery from gas turbines represents a significant potential for sCO2 cycling applications. Table 1 presents the main characteristics of the thermal source adopted in the calculation model.

Table 1 Exhaust Gas Characteristics

Heat Source	2 x AGT on 1 sCO_2
Pressure [bar]	1,04
Temperature [°C]	432
Cold Flue Gas Temperature [°C]	≥ 75
Mass Flow [kg/s]	337
Wet cooling tower parameters:	
Ambient Temperature [°C]	15
Wet Bulb Temperature [°C]	10,8
Approach Temperature [°C]	5
Warm Up Range [°C]	7

2.1 Cycle Architecture

The Regenerative architecture is a general arrangement of the cycle sCO_2, comprising a turbine, recuperator, cooler, and compressor Figure 1. It is a typical closed regenerative Brayton cycle. For most authors, the regenerative cycle is considered the simplest potential architecture.

Due to the difference between the specific heat capacity of the high-pressure stream (2) and low-pressure stream (4), the equipment deal with high irreversibility. Therefore, the temperature of stream (2) will be limited. [13–16].

This effect limits the temperature (T_3) at the heater outlet. Furthermore, this architecture does not allow satisfactory exploitation of the heat source. As a result, a considerable amount of energy is rejected in the stack. These characteristics limit the efficiency of the architecture and its economic performance, especially for WHR.

According to Kim *et al.* [17], in waste heat recovery (WHR), the purpose of cycle optimization is not to maximize the thermal efficiency of the cycle, but to maximize the power output from the waste heat source. Therefore, it is essential to incorporate the thermal efficiency of the cycle (cycle efficiency) and the utilization efficiency of the waste heat (heat recovery efficiency) to maximize the power output of the WHR system from the given heat source (system efficiency).

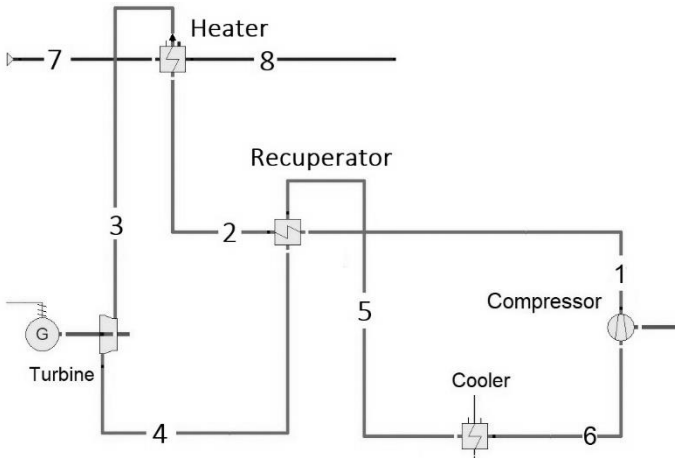

Figure 1 Schematic layout of Regenerative Cycle.

The architectures of sCO_2 cycles characterized by flow-split before heating, such as Recompression, and Preheating cycles, allow for overcoming the Regenerative cycle limitations.

In the Preheating architecture, an additional heater (Preheater) is introduced to the system for heat recovery from the heat source, Figure 2. This architecture splits the CO2 stream into two primary paths after the compression: one through the recuperator and the second through the preheater.

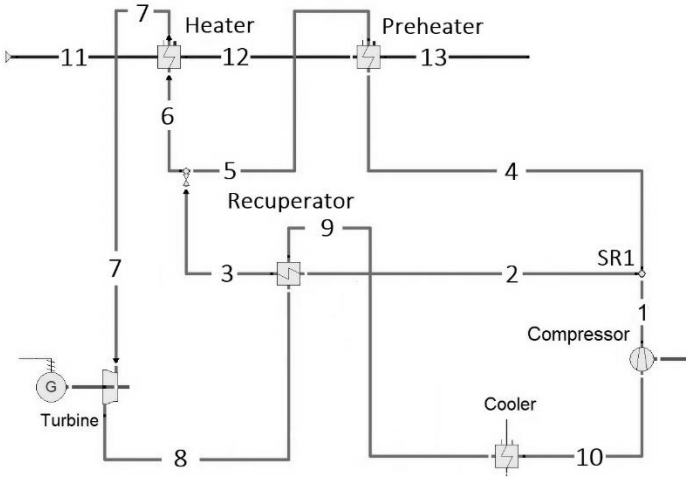

Figure 2 Schematic layout of Preheating Cycle.

In a split flow cycle, the recuperator is divided into low- and high-temperature parts. Each part has different flow rates to accommodate the large variations in the heat capacity of the fluid. If there is an additional low-temperature heat source, it can be used to compensate for the low specific heat of the turbine exhaust stream to minimize the internal irreversibility in the recuperator [2]

The preheating architecture allows better use of the thermal source, recovering heat at two temperature levels (heater and preheater). In addition, the higher mass flow rate ($\dot{m}_{recup_H}$) of the stream (8), which combines the mass flow rate of the

DOI: 10.17185/duepublico/77280

recuperator ($\dot{m}_{recup_C}$) and the preheater ($\dot{m}_{preh.}$), allows for greater heat recovery and increases the equipment's efficiency.

The combined mass flow rate in stream (8) will be represented as:

$$\dot{m}_{recup_H} = \dot{m}_{recup_C} + \dot{m}_{preh.} \quad (1)$$

While the mass ratio between $\dot{m}_{recup_C}$ and $\dot{m}_{recup_H}$ is expressed as:

$$\emptyset = \frac{\dot{m}_{recup_C}}{\dot{m}_{recup_H}} \quad (2)$$

The ratio ($\emptyset$) significantly impacts the recuperator's performance and system optimization.

An in-house calculation tool (OptDesign) developed in MATLAB is used to investigate different sCO2 cycle architectures thermo-economically. The model analyzes the system at cycle and component levels using the Refprop data library to determine the thermodynamic properties. The subroutines determine the heat exchanger design and the turbine isentropic efficiency estimation (related to the equipment inlet's volumetric flow rate). The maximum isentropic efficiency of the turbine is limited to 90%. On the other hand, the efficiency of the pump/compressor is assumed to be 80%.

This study evaluates the operation of supercritical (sCO_2) and transcritical (tCO_2) cycles. In the sCO_2 systems, the compressor inlet temperature is defined as 35°C. While in the tCO_2 system, the minimum temperature is 20°C. Both cycles operate above the critical pressure. The pressure range of the investigation is (75-100 bar) for the low-pressure streams and (200-300) for the high-pressure streams. The minimum temperature difference is limited to 5K in the recuperator and 10K in the heater and preheater.

The OptDesign tool performs a genetic algorithm-based multi-objective optimization (NSGAII) for determining the optimal outcome set.

In this study, two investigations were defined assuming objective functions:

- Maximization of net power and minimization of Fixed Capital Investments (FCI).
- Maximization of Net Present Value and minimization of the Levelized Cost of Energy (LCOE).

The economic analysis of this study addresses the Net Present Value (NPV) methodology and Levelized Cost of Energy (LCOE) as parameters for the thermo-economic evaluation of the investigated sCO2 systems. In addition, the analysis provides an understanding of the effect of the main operating parameters and architectural characteristics on the system's economic performance.

The equipment cost models are based on the literature of [18,19], which explores an extensive analysis of vendor quotes.

The general equation for component cost is determined by:

$$C = aSP^b \times f_T \quad (3)$$

where C is the component cost, a and b are fit coefficients, SP is the scaling parameter, and fT is a temperature correction factor [20]. Table 1 presents the scaling parameters for the primary equipment costs.

Table 1 Summary of the scaling parameters for cost correlation.

Equipment	a	SP		b
Heater	-	UA_{Heater}	$[W_t/K]$	0.7544
Recuperator	49.45	UA_{Recu}	$[W_t/K]$	0.7544
Cooler	32.88	UA_{Cooler}	$[W_t/K]$	0.75
Axial Turbine	182600	P_{mec}	$[MW_t]$	0.5561
Generator	108900	P_e	$[MW_e]$	0.5463
Gearbox	177200	P_{mec}	$[MW_t]$	0.2434
Compressor (centrifugal)	1230000	P_{shaft}	$[MW_t]$	0.3992
Motor	399400	P_e	$[MW_e]$	0.6062

Source: Adapted from[18]

In the NPV analysis, revenue values are calculated annually according to the product's selling price (electricity). The capital expenditure of main equipment (Capex) indicators contemplate the costs of main equipment, site preparation, facility construction, indirect project costs, contingency fees, and others. At the same time, operational expenditure (Opex) determines the fixed and variable costs of the operation as well as maintenance costs.

According to Drennen and Lance [19], these costs contribute significantly to an LCOE estimation; however, they are often ignored. Therefore, the mentioned study contributes a detailed methodology for calculating LCOE.

In this way NPV is defined as:

$$NPV = \sum_{n=1}^{n=20\ years} \frac{Revenue - (Capex - Opex)}{(1 + interestrate)^n} \quad (4)$$

$CAPEX$: Capital expenditure of main components.

$OPEX$: Operational expenditure including operation and maintenance.

The LCOE approach indicates the overall process costs levelized during the economic lifetime of the technology [21]. The LCOE calculation is expressed by:

$$LCOE = \frac{CAPEX \times f_a + OPEX}{P_e \times Hour_{year}} \quad (5)$$

f_a : The discount factor considers both the risk aversion of the investor and the investment distribution over the plant lifetime.

P_e: The electrical power output of the power plant.

$Hour_{year}$: The plant availability.

The LCOE allows quantifying different trade-offs like Capex/Opex or production/annual cost trade-offs [21]. Moreover, this procedure allows economic comparison of different technologies [19].

DOI: 10.17185/duepublico/77280

HEAT EXCHANGER MODEL

The CO_2 thermodynamic properties variation in the vicinity of the critical point is a preponderant aspect of the heat exchangers' design and evaluation of the cycle's operating characteristics.

The Ɛ-NTU, P-NTU, and MTD methods of exchanger heat transfer analysis, assuming the overall heat transfer coefficient (U) as constant and uniform, do not apply to sCO_2 investigation due to highly variable fluid properties.

- PCHE Tool

For the analysis of the sCO_2 operation, a one-dimensional Matlab tool was developed for the heat exchanger performance evaluation. The tool holds a 1-D discretized method, splitting the heat exchanger into 100 nodes. The local thermodynamic properties are determined for each node. The size of individual segments should be sufficiently small so that all fluid properties and other variables/ parameters can be considered constant within each segment [22]. The assessment analyzes a pair of straight semi-circular channels of the heat exchanger. The channel can represent the behavior of the heat exchanger, assuming a uniform flow.

The heat exchanger analysis considers a pressure drop target as an inlet condition while the tool executes the calculation looping to reach the established performance target. The optimization analysis set a 2% pressure drop for each heat exchanger. The unidimensional model was validated using the CFD solver of ANSYS CFX 21.0, and the one-dimensional model demonstrated satisfactory compatibility.

The number of nodes determined in this analysis aims to adequately represent the local effects of the non-linearity of CO_2 properties, mainly in the recuperator. According to [23], the method's main disadvantage is the longer computational time and the iterative temperature derivative of the properties of interest. Therefore, the authors in [18] consider discretizing each heat exchanger model with 20 nodes. The same methodology is adopted by Held [24] for 25 sub-elements.

According to [20], the calculation of overall thermal conductance (UA) based on the log-mean temperature difference (LMTD) for sCO_2 is a poor assumption in many cases, especially for the recuperator and the cooler. This analysis can cause an error in the (UA) prediction of approximately 10% for HTR and 80% for LTR compared to the discretized heat exchanger model.

IDEAL RECUPERATOR

The investigation of [15,16,25] adopts an ideal recuperator model to define the theoretical limit of heat exchanger performance. The theoretical limit is an effect of the differences in thermal properties of both CO_2 streams in the recuperator, in particular specific heat.

As the specific heats of these two flows are different, the change in temperature for one flow will be less than that of the other since the amount of heat is the same for both flows.

The aspects of the recuperator irreversibility are known attributes of sCO_2 operation. Therefore, the present study extends the analysis to explore important features and behavior of the transcritical operation. The lower operating temperatures of the tCO_2 cycle represent a challenge to the recuperator operation since the CO_2 property variations in the vicinity of the critical point are very representative.

Finally, this analysis encompasses the aspects of different mass flow rates between streams in the recuperator. The splitting flow architectures are practical alternatives to overcome the irreversibility limitation in the recuperator. However, the operating ranges of the tCO_2 cycles lead to significant changes in the CO_2 properties. These different characteristics result in additional criteria that are significant for the recuperator analysis, especially in thermo-economic considerations.

The present analysis proposes a similar approach considering an ideal heat exchanger with an infinity length. However, for a more meaningful analysis, considers the recuperator terminal temperature difference (LTTD) as 10 K, defined in equation 6.

$$LTTD = T_9 - T_2 \tag{6}$$

Therefore, the terminal temperature difference (UTTD) express the temperature difference between the stream (3) and stream (8). The UTTD minimum defined in the model is 5K.

$$UTTD = T_3 - T_8 \tag{7}$$

The study of [15,16,25] uses the recuperator temperature effectiveness concept to determine how close the cold outlet temperature T_3 is to the hot inlet T_8 in an ideal recuperator. The temperature effectiveness is defined as:

$$TE = \frac{T_3 - T_2}{T_8 - T_2} \tag{8}$$

This concept does not apply to the recuperator calculation model for non-ideal equipment analysis (finite length). The realistic analysis of the heat exchangers follows the effectiveness equation proposed in [22].

The parametric analysis estimates the temperatures T_8 and T_2 for each operating pressure evaluated in the range: of 7.5-9.5 MPa (low pressure) and 20-30 MPa (high pressure), with a 0.1 MPa step.

The turbine inlet temperature will be T_1= 634 K throughout the analysis. At the same time the compressor inlet temperature is set to T_{10}=308 K in sCO_2 cycles and T_{10}=293 K in tCO_2 systems. The efficiencies of the turbine ($\eta_T = 0.9$) and the compressor ($\eta_C = 0.8$) are constant. For instance, the temperature range T_2 is (314 to 323 K) at the tCO_2 and (337 to 419 K) at the sCO_2 cycle.

Figure 3 represents this operating range for the inlet side of the recuperator (lower temperature side). Furthermore, the specific heat capacity shows a significant variation, especially in transcritical cycle design.

DOI: 10.17185/duepublico/77280

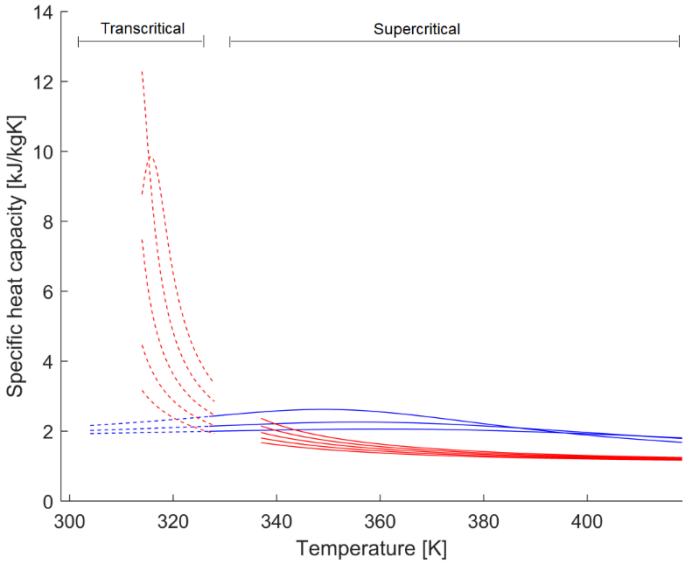

Figure 3: CO_2 specific heat capacity profile at the transcritical and supercritical recuperator range of operation.

RESULTS

Parametric Analysis

The parametric analysis of the idealized recuperator aims to investigate various operating conditions of the sCO_2 and tCO_2 cycles. The analysis based on the idealized recuperator model uses the one-dimensional PCHE tool to evaluate the thermodynamic properties of each operating condition. The mass and energy balance defines the temperature distribution along the equipment. The model determines the heat capacity characteristics, and the temperature difference between the recuperator flows over 100 calculation sections representing the equipment. This approach allows for a quick investigation of several operating conditions as critical characteristics of the recuperator's operation. In particular, the analysis aims to investigate the effect of the nonlinear behavior of the CO_2 properties on the characteristics of the recuperator, especially in transcritical operation.

- **Supercritical cycle**

The contour diagram in Figure 4 represents the parametric analysis of the idealized recuperator. The independent variable (temperature effectiveness) levels are presented in a color scale, referring to each pair of the operating pressure (high pressure and low pressure) evaluated.

The results of 4.a referring to the Regenerative architecture (Ø=1) at supercritical condition point to the well-known characteristic of sCO_2 cycles: the remarkable irreversibility of the equipment due to the imbalance of heat capacity.

For the analysis's boundary conditions, the recuperator's temperature effectiveness was restricted to 0.54-0.64. A widely discussed alternative to overcome this limitation is employing different levels of mass flow between the equipment streams. Thus, Figure 4b presents the analysis of increasing the mass flow rate of the low-pressure stream (Ø=0.7). The results point to a significant increase in temperature effectiveness (0.84-0.98) for the same independent variables evaluated.

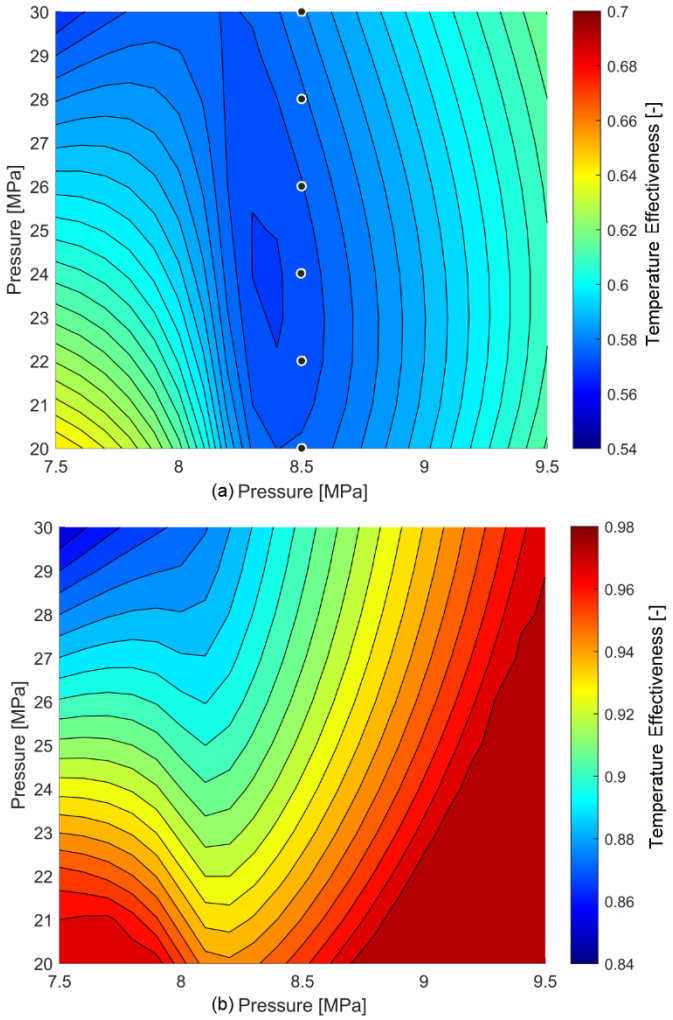

Figure 4: Temperature effectiveness of the sCO_2 idealized recuperator. (a) $\emptyset = 1$. (b) $\emptyset = 0.7$.

Figure A1 (Annex A) points out the characteristics of the operation referring to the sCO_2 cycle and Ø=1, with low pressure of 85 bar and six high-pressure levels from 200 to 300 bar (points represented in graph 4.1a). Segment 1 refers to the recuperator inlet, low-temperature side. In this configuration, the higher heat capacity value on the heat exchanger's high-pressure side restricts heat transfer, limiting the output temperature of the high-temperature side.

Similarly, the operation with Preheating architecture, Figure A2 (Annex A), allows a better balance of the heat capacity, increasing the equipment's effectiveness and allowing higher temperature at the output. Its indicated by the lower temperature difference. The temperature difference distribution is not linear due to the characteristics of the CO_2 properties combined with the different mass flow rates.

DOI: 10.17185/duepublico/77280

- **Transcritical Cycle:**

The parametric analysis proposed is particularly insightful when evaluating the characteristics of the transcritical operation. Figure 5 presents the distribution of properties across the exchanger for the same pressure conditions as the previous analysis, whereas for the transcritical cycle.

Furthermore, Figure 5a presents the results of the tCO_2 with Ø=1. Similarly to the sCO_2 cycle, the effects of the higher specific heat capacity in the high-pressure stream lead to the same irreversible characteristics.

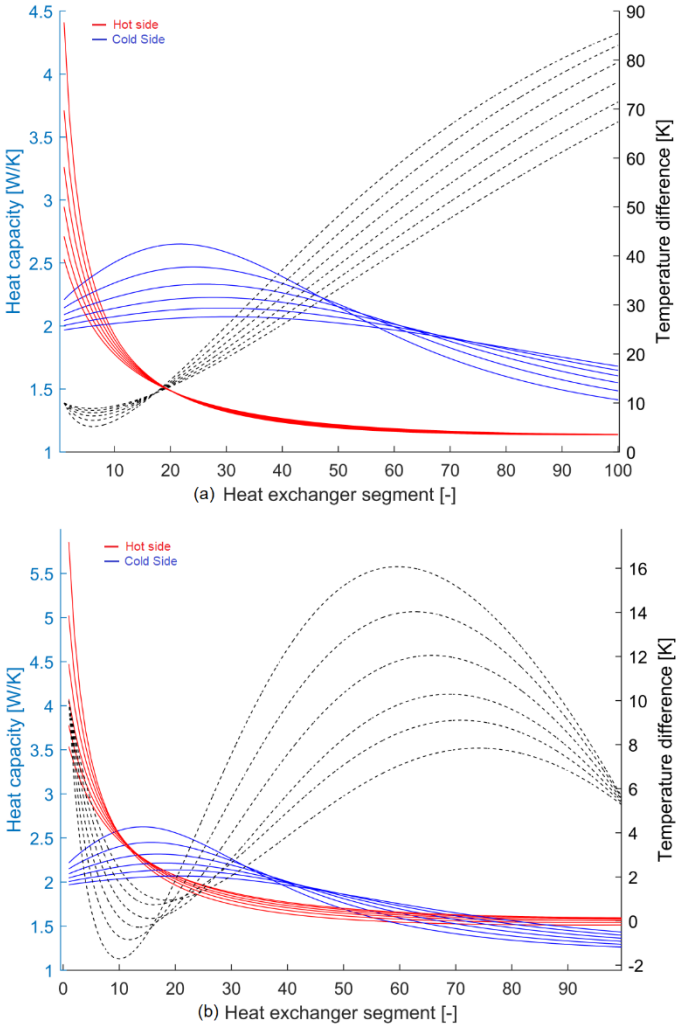

Figure 5: Properties distribution along the tCO_2 idealized recuperator. (a) $\emptyset = 1$. (b) $\emptyset = 0.7$.

Although at the recuperator inlet, there is a remarkable increase in the specific heat capacity on the low-pressure side. This characteristic is associated with the influence of the vicinity of the critical point. As a result, the deviation of the temperature difference curve in the inlet region (segments 1 to 10) of the recuperator is noticeable.

Consequently, a higher mass flow rate of the low-pressure stream, as represented in Figure 5b (0.7), accentuates the heat capacity difference in this region. Thus the temperature difference at the recuperator tends to zero, as indicated by the temperature distribution. This characteristic implies an exponential increase in the heat exchange area. Similarly, as indicated, some operating conditions tend to pinch point violations, which is not thermodynamically possible.

Figure 6 shows the contour diagram for the analysis of the transcritical operation. The gray areas indicate the operating conditions leading to a pinch-point violation, which is, therefore, thermodynamically unacceptable.

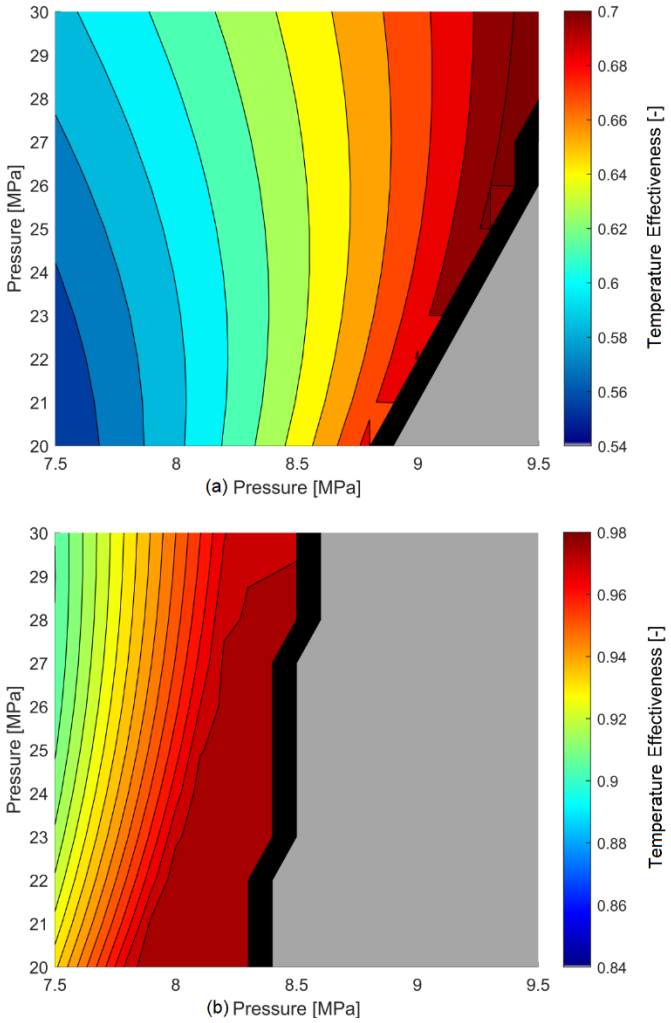

Figure 6: Temperature effectiveness of the tCO_2 idealized recuperator. (a) $\emptyset = 1$. (b) $\emptyset = 0.7$.

It is notorious that the temperature effectiveness is higher under transcritical operating conditions. However, especially in the split-flow architecture (Figure 6b), a significant portion of the operating conditions lead to pinch point violation internally in the exchanger.

The parametric study reveals significant features for the transcritical operation analysis. Foremost, the split flow characteristics allow for less irreversibility in the recuperator. Therefore providing a higher temperature at the recuperator outlet enhances the cycle's performance. However, unlike the

DOI: 10.17185/duepublico/77280

supercritical operation, the characteristics of higher specific heat capacity in the low-pressure stream are exacerbated by the higher mass flow of this stream. Then, it leads to a pinch temperature inside the equipment while restricting the range of possible operating conditions. The temperature pinch refers to a local temperature difference within an exchanger that is lower than either of the two terminal temperature differences and is minimum in the equipment [22].

Figure 7 shows important features in the recuperator analysis for this operating condition. The heat exchanger evaluation considered a dimensionless mass flow during the analysis. Therefore, the overall thermal conductance, heat transferred, and heat transferred area at the recuperator calculated by the PCHE tool are demonstrated in representative terms, products of these parameters by a factor (ft).

Figure 7a presents the minimal temperature differences in the recuperator inlet regions. It can be observed that the pinch temperature decreases with increasing low pressure, until the pinch point violation conditions.

It is noticeable that the temperature pinch inside the equipment is considerably lower than LTTD (10K). Thus, these operating conditions suggest a significantly higher overall conductance.

Therefore, the increase in overall conductance (Figure 7c) is more closely related to the decrease of the temperature difference in the pinch point region than to the total heat absorbed at the equipment (Figure 7b).

The analysis of the area factor according to the one-dimensional analysis of the recuperator shows the same outcome (Figure 7d). Similarly, the significant increase in UA relates to the increase in the heat exchange surface area due to the enlargement of the pinch-point effect, which requires a larger heat transfer area.

An operation at the high-pressure 280 bar leads to UA values 4.4 times higher at low-pressure 85 bar than at 75 bar, even though this indicates better recuperator effectiveness.

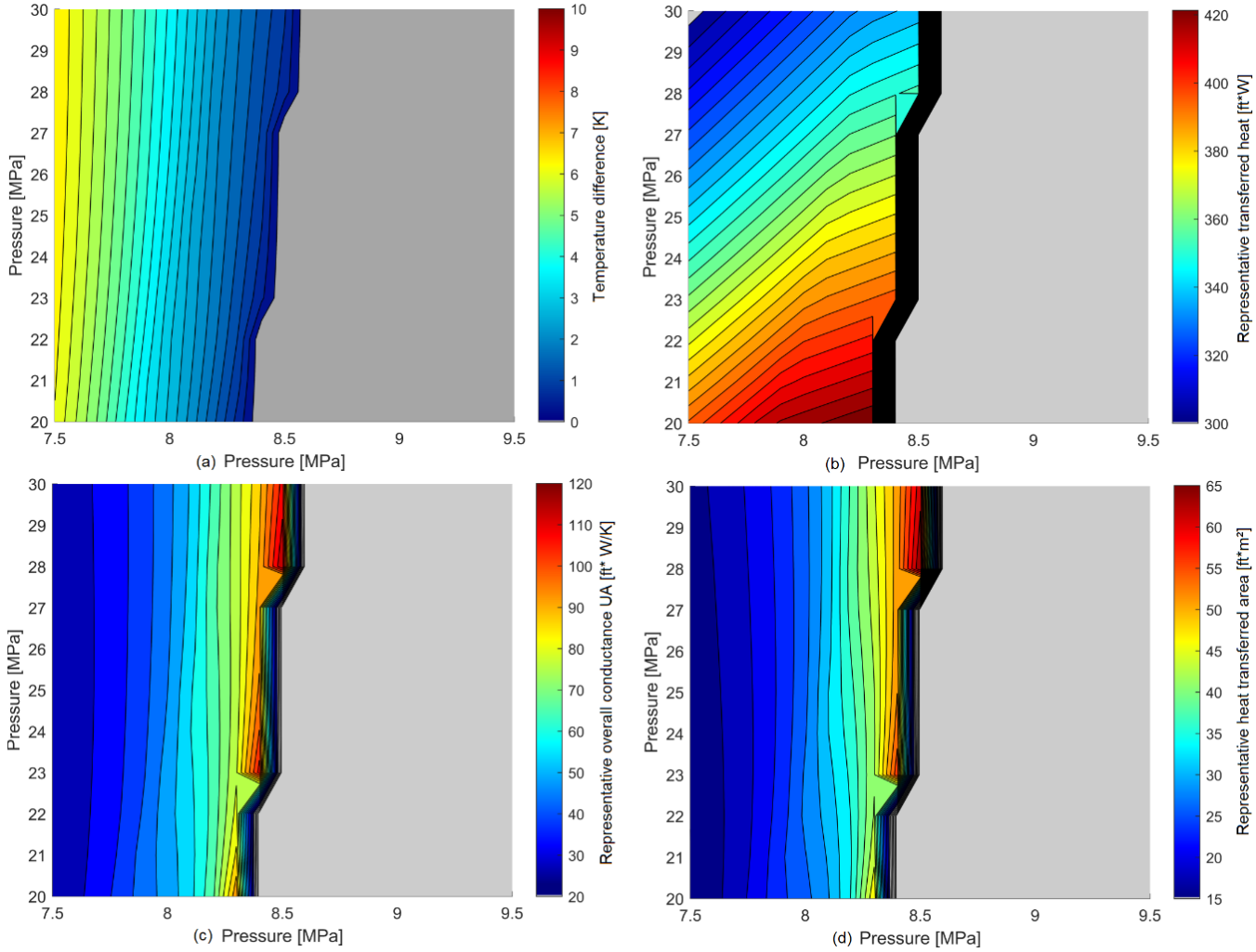

Figure 7: Features of the idealized tCO2 recuperator indicated in the parametric analysis. (a) Minimal temperature difference. (b) Representation of transferred heat. (c) Representation of overall conductance. (d) Representation of transferred area.

DOI: 10.17185/duepublico/77280

In addition, although this provides 12.3% more heat recovery, this operating condition leads to a pinch point of 0.7 K, in contrast to a pinch point of 6.5 K at 75 bar.

The effects of mass ratio on preheating architecture provide conflicting results for recuperator design. While reducing ∅ allows for a reduction in irreversibility, it can also lead to a pinch-point, a significant increase in the heat exchanger area, and, consequently, an increase in equipment cost.

Furthermore, the performance gains expected by the different mass ratios in the recuperator can drastically restrict the design operating range of the equipment and limit the off-design operations.

Therefore, the effects of the nonlinearity of the CO_2 properties enhanced by the mass ratio by the Preheating transcritical cycle demand a more complex analysis for cycle optimization. Thess effects has a relevant impact on equipment analyses and system optimization.

MULTIOBJETICVE OPTIMIZATION

This study performed a multiobjective optimization analysis of the sCO_2 cycle for waste heat recovery based on different thermo-economic criteria comparing two sets of the objective function:

1-Maximization of NPV and minimization of LCOE.

2- Maximization of net power and minimization of Fixed Capital Ivestiment (FCI).

The results demonstrate that the economic analysis criteria are crucial for defining the optimal operating conditions. The Pareto's frontier from the optimization adopting the first set of objective functions corresponds to a fraction of the optimal results of the net power analysis (set 2). Therefore, the operating conditions of the first analysis are not associated with the highest power generation of the cycle.

Figure 8 presents the multiobjective optimization results with the Pareto for the sCO_2 and tCO_2 systems. The most prominent frontier, with power generation between 31.9-35.7, corresponds to the tCO_2 cycle designs.

Therefore, the scope of the present analysis encompasses range-I (which allows the best thermo-economic performance of the system) up to the designs with the highest power generation (range-III). Furthermore, the analysis aims to demonstrate which parameters influence the economic depreciation at the higher power generation designs. A parametric evaluation of the results indicates that the operating conditions of the recuperator have a decisive effect on the best thermo-economic performance.

Tables 3 and 4 present the main operating parameters of the transcritical and supercritical cycle designs. A previous study evaluates a wider range of thermo-economic results and concludes that designs with lower power generation than Range-1 demonstrate lower thermo-economic performance [26].

The transcritical operation generally provides a higher potential for the investigated operating conditions. The optimum results for the thermo-economic analysis (Range-I) indicate that the transcritical system allows more efficient cycles, with higher net power (up to 20.2%) and three times higher NPV associated with lower LCOE (10.7% lower) compared to the sCO2. Furthermore, the tCO2 design is generally associated with lower compression work and higher power in the turbine as it operates with lower minimum temperatures.

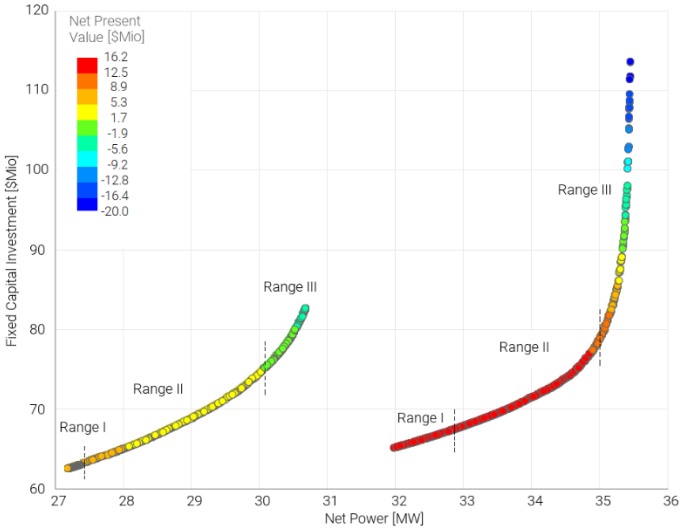

Figure 8 Optimization results of sCO_2 and tCO_2 operation.

The parametric analysis of the results of the transcritical operation, Table 3, indicates that the net power on Range I (31.9 to 32.8 [MW]) is, on average, 10% inferior to the maximum net power of Range III (35 to 35.7 [MW]). However, the gain in net power and thermal efficiency of the cycle is associated with a significant increase in equipment cost, consolidating in the decrease of NPV and increased LCOE.

Table 3 Parameters of tCO_2 optimization results.

		Range-I	Range-II	Range-III
Net Power	[MW]	31.9–32.8	32.7 - 35	35 – 35.7
NPV	[Mio$]	16.2	16.1–0.2	10.1–(-20.0)
LCOE	[$/MWh]	34.1–34.2	34.2–37.0	37.1–48.9
Efficiency	[%]	26.2–26.9	26.9–28.7	28.8–29.1
Pressure	[Bar]	267–272	258–280	249–258
Temp. T1	[K]	633–634	617–634	609–618
UTTD	[K]	14–10	10–5	5
LTTD	[K]	25–24	24–10	10 –8
$\dot{m}_{recup_C}$	[kg/s]	249-252	248-316	318-342
$\dot{m}_{preh.}$	[kg/s]	160-165	162–171	159-163
∅ Ratio	[-]	60.3-60.9	59.3-66.0	66.2-68.2
UA_{recup}	[MW/K]	3.62-4.2	4.2-13.7	14-57.4
UA_{heater}	[MW/K]	2.0–2.2	2.1-2.8	2.4-2.5
$UA_{preheater}$	[MW/K]	1.60-1.9	1.8-2.6	2.3-2.4

The increase in the thermodynamic performance of the system (range-I to range-III) is mainly associated with the higher heat recovery in the recuperator. For instance, at the tCO_2 operation, the heater has a 2.1% increase in absorbed heat, while in the recuperator, it represents 35.3%. This higher exploitation also evidences the decrease in the UTTD and LTTD.

DOI: 10.17185/duepublico/77280

Thus, the reduction of LTTD (24°C to 10°C) and UTTD (10°C to 5°C) at range-II results in up to 3.2 times higher UA_{recup}. While in range-III, reducing LTTD from (10°C to 7°C) results in 13.6 times higher UA. In this last range, the combined increase of UAheater and UApreheater is only 15.6%.

The increase in UA_{recup} in these ranges is largely responsible for the equipment cost rise. In this way, there is a reduction in NPV in Range-II from 16.1 Mio$ to -0.2 Mio$. While in range-III, the exponential increase in recuperator cost would result in NPV of -20Mio$. Similarly, the LCOE values increase from (34.1-34.2) to (37.1- 48.9).

The exponential increase of UA_{recup} in the range-III frontier is associated with the pinch point effect in the equipment. This characteristic is mainly responsible for the exponential increase in system and LCOE costs, and the decrease in NPV.

The effect of the internal pinch point in the recuperator becomes evident in the tCO_2 designs at range-III. Although these designs range the LTTD between 7 and 10, the minimum temperature difference occurs inside the equipment, as evidenced by the parametric analysis. Thus, the pinch temperatures in these cases vary between 5 and 0.5. Consequently, once the temperature difference in the equipment tends to zero, the heat exchange surface of the equipment would tend to infinity.

Therefore, this reflects in the characteristic of the exponentially increasing equipment cost. The NPV decreases from 9.9 $Mio for a net power of 35 MW to -20 $Mio for a net power of 35.7 MW. Thus these conditions are not techno-economically realistic.

The sCO_2 cycle optimization results described in Table 4 follow the same characteristics of the previous analysis for the tCO_2 system. The range-I compose the optimal designs in NPV maximization and LCOE minimization.

Table 4 Parameters of sCO_2 optimization results.

		Range-I	Range-II	Range-III
Net Power	[MW]	27.1–27.3	27.4-30.2	30.2 – 30.7
NPV	[Mio$]	5.42-5.45	5.41-0.54	0.54–(-4.0)
LCOE	[$/MWh]	38.2-38.3	38.3-40.8	40.7-40.9
Efficiency	[%]	22.3-22.5	22.5-24.9	24.7-25.2
Pressure	[Bar]	275-276	236-280	220-240
Temp. T1	[K]	634-635	604-640	594-605
UTTD	[K]	12–10	10-5	5.0
LTTD	[K]	25–24	25-10	10 – 5.0
$\dot{m}_{recup_C}$	[kg/s]	262–263	258-369	369- 424
$\dot{m}_{preh.}$	[kg/s]	155–159	152-192	188 - 196
∅ Ratio	[-]	62.1-62.4	60.9-66.0	65.9-68.7
UA_{recup}	[MW/K]	3.3 - 3.4	3.3-9.3	9.3-14.5
UA_{heater}	[MW/K]	2.0–2.1	2.1–2.6	2.1–2.2
$UA_{preheater}$	[MW/K]	1.3–1.4	1.2-3.6	3.6-4.2

Similarly, the power increase from range-I is accompanied by better thermodynamic performance, although penalizing the techno-economic criteria. The NPV values decrease from (5.42 to 5.45 Mio$) to (0.54 to -4.0 Mio$) in range-III. As well as, LCOE increase from (38.2 to 38.3 $/MWh) to (40.7 to 40.9 $/MWh). As in the previous analysis, these characteristics also result from the higher heat recovery at the recuperator.

Thus, as a common characteristic between both cycles, the increase in net power and thermodynamic performance is associated with more intensive use of the recuperatort. However, these designs are associated with higher costs and do not configure the optimal results of the thermo-economic analysis.

The higher internal heat recovery of the cycle correlates to systems with higher mass flow rates. In order to accommodate these characteristics, the designs indicate an increase in the recuperator's mass ratio, a decrease in temperature and pressure at the main heater outlet, a decrease in specific work, and modify the cost ratio with other heat exchangers.

These characteristics will be discussed in the following topics.

- Specific net power

Range-I designs converge to operate at higher turbine inlet pressures and temperatures than in the range (II, III) designs. Meanwhile, the operating conditions occur at lower mass flow rates and larger temperature differences in the heat exchangers. These characteristics provide a better thermodynamic and economic performance ratio.

The net power gain in the range (II, III) increasing the flow rate in the recuperator path restricts the heater's and preheater's operating conditions. Thus, high pressure and temperature operation conditions are not achievable.

Therefore, maximizing the recuperator exploitation demands lower pressure and temperature operations at the heater outlet. Thus, although these designs provide higher power generation, they conduct lower specific power.

- Pinch Point Restriction:

The increase of the CO_2-specific heat capacity in the vicinity of the critical region directly impacts the recuperator operating conditions. This characteristic is especially aggravated in Preheating architecture at transcritical operation. Therefore, the maximization of the recuperator usage tends to the temperature pinch occurrence and pinch-point violations.

Thus, the designs of range-III imply an exponential increase in the UA in the recuperator. The one-dimensional analysis of the recuperator evidence that the temperature difference between the streams in the recuperator tends to zero under these operating conditions.

Although these operating conditions (range-III) are thermodynamically accepted, they would be impractical. However, when the equipment analysis does not correctly consider the properties variation, it may not observe these characteristics, which leads to erroneous decision-making in cycle evaluation

- Matching performance of recuperator and preheater:

The maximal use of the recuperator and the highest exploitation of the heat source characterize the higher net power achieved in range-III. In this way, the residual gases from the gas turbine leave the preheater with the minimum temperature established in the calculation model (348K).

DOI: 10.17185/duepublico/77280

However, the increase of the mass flow of the recuperator path is higher than that of the preheater. For instance, at the tCO_2, the split flow ratio decreases from 0.65 at range-I to 0.46 at range-III. Similarly, the rate reduces from 0.60 to 0.45 in the sCO_2.

In this way, it is evident that the operating conditions of the recuperator and the preheater stream are complementary for better cycle performance. However, they compete regarding the use of the thermal source.

The increase in the mass flow of the recuperator path associated with higher power generations implies lower temperatures of the thermal source at the heater's outlet (stream 12), decreasing the availability of energy in the preheater. Thus, due to the lower temperature differences in the preheater, the specific cost of the equipment increases.

The reduction of the CO_2 operating pressure and temperature at the heater outlet mentioned before is related to accommodating the operating conditions of the preheater stream to the increased mass $\dot{m}_{recup_C}$.

- Mass flow Ratio:

The parametric analysis pointed out how the imbalanced flow levels in the recuperator can compensate for the different CO_2 properties in the recuperator leading to improved performance, but can also aggravate certain characteristics leading to unacceptable operating conditions.

The multiobjective optimization has highlighted in the tCO_2 system that the effects of pinch temperature decrease inside the recuperator are the major responsible for the exponential increase of costs. Thus, it is evident that the mass flow ratio significantly impacts the system design analysis.

Therefore, this analysis evaluates the effects on cycle performance of varying the mass flow ratio in the recuperator for the optimal thermal-economic performance design (DP-Range 1, Ø=0.60; Net Power= 32.8 MW; NPV= 16.2 Mio$) and the highest net power generation design (DP-Range 3, Ø=0.68; Net Power= 35.4 MW; NPV= -20.0 Mio$). The operating pressure and temperature levels at the turbine inlet were maintained for these reference design conditions. Figure 9 presents the results.

In the DP-Range1 design, the increase from Ø=0.60 to Ø=1 negatively impacts net power and economic performance (NPV and LCOE). The net power reduction is associated with the irreversibility increase in the recuperator and less heat recovery in the preheater.

However, for the DP-Range 3 design point, the increase in mass flow ratio (Ø) also leads to a net power reduction, although initially, it improves economic performance.

The better match of mass flow ratio modifies the heat capacity ratio at the recuperator's inlet, avoiding the pinch-point effect. Therefore, the novel operation condition would result in a net power of 30.0 MW (as opposed to 35.4 MW) and an NPV value of 8.71 Mio$.

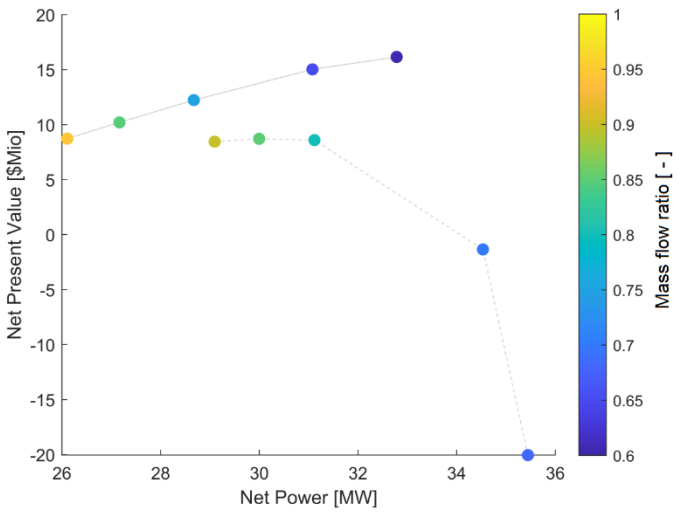

Figure 8 Mass flow ratio impact on cycle performance.

CONCLUSION

The study presents a parametric analysis to investigate the effect of the non-linear behavior of the CO_2 properties on the recuperator characteristics. The approach analyzes supercritical and transcritical CO_2 cycles in a Preheating architecture.

In general, the operation with different mass flow levels in each stream of the recuperator, compensates the differences in the CO_2 properties between the low and high-pressure flow, reducing irreversibility in the equipment.

Although these characteristics contribute to conflicting effects in transcritical operations. The investigation of the transcritical operation points out that while the split flow reduces irreversibility, it can also conduct a lower temperature pinch inside the equipment, a significant increase in the heat exchanger area and consequently, an increase in equipment cost.

The study describes a thermo-economic optimization of both systems for waste heat recovery from a gas turbine (medium-temperature thermal source). According to the multiobjective optimization, the transcritical operation allows a 20.1% improvement in net power, 10.7% reduction of LCOE and three times higher NPV, compared to the supercritical cycle. Furthermore, the analysis indicates that maximizing the recuperator's heat recovery leads to higher power generation and more efficient cycles. However, the highest net power range designs are associated with lower specific work, higher specific costs, and unfavorable economic performance for both cycles.

In the tCO_2 system, the designs that provide the best thermal-economic performance range between 31.9 and 32.8 MW of net power. An 8.8% increase in net power from this range entails a 69% higher cost. Mostly due to the costs of the recuperator. As a result, NPV values decrease dramatically from the optimal result of 16.2 Mio$ to negative values.

In addition, to accommodate and allow for more significant recuperator exploitation and consequently increased efficiency, the designs operate with lower pressure and temperature at the turbine inlet, which decreases the net power by 11.1%. In this

DOI: 10.17185/duepublico/77280

range, the characteristics of the recuperator also negatively impact the performance of the preheater.

The parametric analysis followed by multiobjective optimization indicates that the operating characteristics of the recuperator are crucial for optimal system performance. While for the transcritical cycle, the effects of the non-linear CO_2 properties on the recuperator are a challenge to system optimization and off-design operation.

ACKNOWLEDGEMENTS

These investigations were conducted as part of the research project CARBOSOLA. The authors would like to thank the German Federal Ministry of Economics and Energy (BMWi) for the financial support as per resolution of the German Bundestag under grant numbers 03EE5001A (Siemens) and 03EE5001B (TU Dresden). The authors alone are responsible for the content of this paper.

NOMENCLATURE

C	*Component Cost*
CAPEX	*Capital expenditure of main C*
DC	*Direct costs*
FCI	*Fixed Capital Investment*
HT	*High temperature*
HP	*High pressure*
HTR	*High temperature recuperator*
Hx	*Heater*
IC	*Indirect cost*
LCOE	*Levelized Cost of Energy*
LMTD	*Log Mean Temperature Difference*
LTTD	*Lower Terminal Temperature Difference*
LP	*Low pressure*
LT	*Low temperature*
LTR	*Low temperature recuperators*
$\dot{m}$	*Mass flow*
NPV	*Net Present Value*
OPEX	Operational expenditure
PEC	*Purchased Equipment Cost*
Pe	*Eletrical power output*
SR	*Split ratio*
U	overall heat transfer coefficient
UA	*Overall thermal conductance*
UTTD	*Upper Terminal Temperature Difference*
WHR	*Waste Heat Recovery*

REFERENCES

[1] Huck P, Freund S, Lehar M, Peter M. Performance comparison of supercritical CO2 versus steam bottoming cycles for gas turbine combined cycle applications. 5th Int Symp - Supercrit CO2 Power Cycles 2016.

[2] Kim YM, Sohn JL, Yoon ES. Supercritical CO2 Rankine cycles for waste heat recovery from gas turbine. Energy 2017;118:893–905. https://doi.org/10.1016/j.energy.2016.10.106.

[3] Li B, Wang S sen, Wang K, Song L. Comparative investigation on the supercritical carbon dioxide power cycle for waste heat recovery of gas turbine. Energy Convers Manag 2021;228. https://doi.org/10.1016/j.enconman.2020.113670.

[4] Ancona MA, Bianchi M, Peretto A, Torricelli N, Branchini L, Pascale A De, et al. Power Plants for Energy Harvesting in Industrial Gas Turbines 2021.

[5] Musgrove G, Sullivan S, Shiferaw D, Fourspring P, Chordia L. 8-Heat exchangers. Elsevier Ltd; 2017. https://doi.org/10.1016/B978-0-08-100804-1.00008-6.

[6] Guo J. Design analysis of supercritical carbon dioxide recuperator. Appl Energy 2016;164:21–7. https://doi.org/10.1016/j.apenergy.2015.11.049.

[7] Kwon JS, Bae SJ, Heo JY, Lee JI. Development of accelerated PCHE off-design performance model for optimizing power system operation strategies in S-CO2 Brayton cycle. Appl Therm Eng 2019;159:113845. https://doi.org/10.1016/j.applthermaleng.2019.113845.

[8] Xie J, Liu D, Yan H, Xie G, Boetcher S. A review of heat transfer deterioration of supercritical carbon dioxide flowing in vertical tubes- Heat transfer behaviors, identification methods, critical heat fluxes, and heat transfer correlations.pdf. Int J Heat Mass Transf 2019;149.

[9] Marchionni M, Chai L, Bianchi G, Tassou SA. Numerical modelling and performance maps of a printed circuit heat exchanger for use as recuperator in supercritical CO2 power cycles. Energy Procedia 2019;161:472–9. https://doi.org/10.1016/j.egypro.2019.02.068.

[10] Cabeza L, Gracia A de, Fernández I, Farid M. Supercritical CO2 as heat transfer fluid: A review. Appl Therm Eng 2017;125:799–810.

[11] Xu XY, Wang QW, Li L, Chen YT, Ma T. Study on thermal resistance distribution and local heat transfer enhancement method for SCO2-water heat exchange process near pseudo-critical temperature. Int J Heat Mass Transf 2015;82:179–88. https://doi.org/10.1016/j.ijheatmasstransfer.2014.11.029.

[12] Xiao G, Xing K, Zhang J, Yang T, Ni M, Cen K. Heat Transfer Characteristics of Sco2 and Dynamic Simulation Model of Sco2 Loop. 3 Rd Eur Supercrit CO2 Conf 2019:1–11. https://doi.org/10.17185/duepublico/48881.

[13] Feher EG. The Supercritical Thermodynamic Power Cycle. Energy Convers 1967;8:85–90.

[14] Moisseytsev A, Sienicki JJ. Investigation of alternative layouts for the supercritical carbon dioxide Brayton cycle for a sodium-cooled fast reactor. Nucl Eng Des 2009;239:1362–71. https://doi.org/10.1016/j.nucengdes.2009.03.017.

[15] Dostal V, Hejzlar P, Driscoll MJ. High-performance supercritical carbon dioxide cycle for next-generation nuclear reactors. Nucl Technol 2006;154:265–82. https://doi.org/10.13182/NT154-265.

DOI: 10.17185/duepublico/77280

[16] Moisseytsev A. Passive Load Follow Analysis of the STAR-LM and STAR-H2 Systems. 2003.
[17] Kim YM, Lee YD, Ahn KY. Parametric study of a supercritical CO2 power cycle for waste heat recovery with variation in cold temperature and heat source temperature. Energies 2021;14. https://doi.org/10.3390/en14206648.
[18] Weiland NT, Lance BW, Pidaparti S. SCO2 POWER CYCLE COMPONENT COST CORRELATIONS FROM DOE DATA SPANNING MULTIPLE SCALES AND APPLICATIONS. Proc ASME Turbo Expo 2019 Turbomach Tech Conf Expo 2019:1–17.
[19] Drennen T, Lance B. An integrated techno-economic modeling tool for sCO2 Brayton cycles. 2019.
[20] Weiland N, Thimsen D. A Practical Look at Assumptions and Constraints for Steady State Modeling of sCO2 Brayton Power Cycles. 5th Int Symp - Supercrit CO2 Power Cycles 2016:1–14.
[21] Zhao Q. Conception and optimization of supercritical CO2 Brayton cycles for coal-fired power 2019.
[22] Shah RK, Sekulic DP. Fundamentals of Heat Exchanger Design. 2003.
[23] Hoopes K, Sánchez D, Crespi F. A NEW METHOD FOR MODELLING OFF-DESIGN PERFORMANCE OF sCO2 HEAT EXCHANGERS WITHOUT SPECIFYING DETAILED GEOMETRY. 5thInternational Symp - Supercrit CO2 Power Cycles 2016:1–14.
[24] Held TJ. Supercritical CO2 cycles for gas turbine combined cycle power plants. Power Gen Int 2015.
[25] Mylavarapu SK. Design, Fabrication, Performance Testing, and Modeling of Diffusion Bonded Compact Heat Exchangers in a High-Temperature Helium Test Facility. Ohio State University, 2011.
[26] Gotelip T, Gampe U, Glos S. Optimization strategies of different SCO2 architectures for gas turbine bottoming cycle applications. Energy 2022;250:123734. https://doi.org/10.1016/j.energy.2022.123734.

 DOI: 10.17185/duepublico/77280

ANNEX A

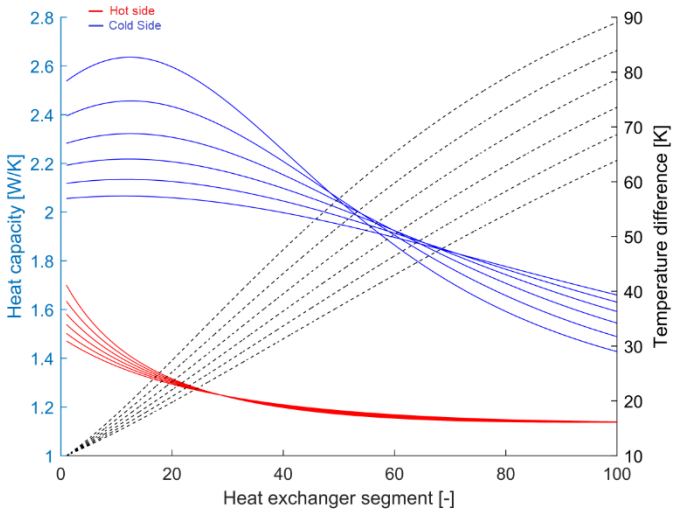

Figure A1: Properties distribution along the sCO_2 idealized recuperator ($\emptyset = 1$).

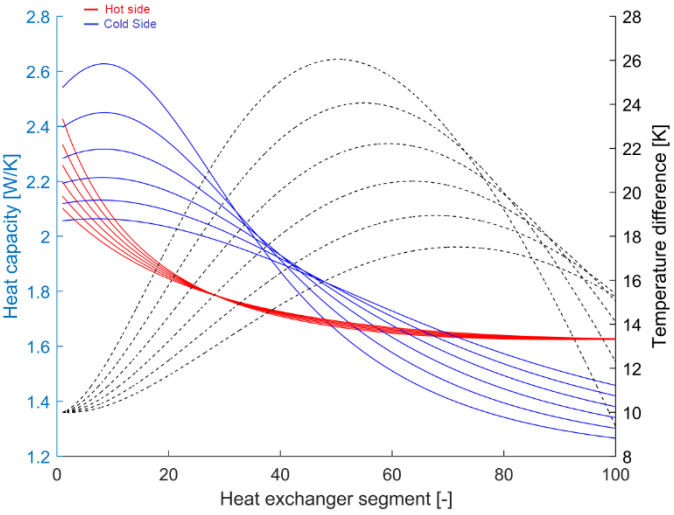

Figure A2: Properties distribution along the sCO_2 idealized recuperator ($\emptyset = 0.7$).

DOI: 10.17185/duepublico/77280

DOI: 10.17185/duepublico/77280
URN: urn:nbn:de:hbz:465-20230427-120203-8